Vision Research 73 (2012) 30–39

Contents lists available at SciVerse ScienceDirect

Vision Research

journal homepage: www.elsevier.com/locate/visres

Recovery of peripheral refractive errors and ocular shape in rhesus monkeys (*Macaca mulatta*) with experimentally induced myopia

Juan Huang, Li-Fang Hung, Earl L. Smith III *

College of Optometry, University of Houston, Houston, TX, United States
Vision CRC, Sydney, Australia

ARTICLE INFO

Article history:
Received 12 June 2012
Received in revised form 3 September 2012
Available online 28 September 2012

Keywords:
Myopia
Form deprivation
Peripheral refractive error
Peripheral hyperopia
Ocular shape

ABSTRACT

This study aimed to investigate the changes in ocular shape and relative peripheral refraction during the recovery from myopia produced by form deprivation (FD) and hyperopic defocus. FD was imposed in six monkeys by securing a diffuser lens over one eye; hyperopic defocus was produced in another six monkeys by fitting one eye with −3 D spectacle. When unrestricted vision was re-established, the treated eyes recovered from the vision-induced central and peripheral refractive errors. The recovery of peripheral refractive errors was associated with corresponding changes in the shape of the posterior globe. The results suggest that vision can actively regulate ocular shape and the development of central and peripheral refractions in infant primates.

1. Introduction

Several lines of evidence indicate that ocular growth and refractive development in a wide range of animal species are regulated by visual feedback associated with the eye's refractive state (Smith, 2011; Wallman & Winawer, 2004). The most direct evidence comes from lens-compensation experiments that have shown that optically imposed changes in the eye's effective refractive state produce predictable changes in ocular growth and refractive development (Howlett & McFadden, 2009; Hung, Crawford, & Smith, 1995; Schaeffel, Glasser, & Howland, 1988; Schaeffel & Howland, 1991; Shaikh, Siegwart, & Norton, 1999; Smith & Hung, 1999; Whatham & Judge, 2001). For instance, in response to relative hyperopic defocus optically imposed via negative-powered lenses, the eyes of developing animals consistently elongate and develop degrees of myopia that compensate for the induced optical error. On the other hand, relative myopic defocus imposed by positive lenses slows axial growth and produces hyperopic refractive errors and, again, over a range of moderate lens powers the eye's final refractive error is correlated with the power of the treatment lens.

Another powerful line of evidence that emmetropization is regulated by visual feedback comes from experiments in which it has been observed that young animals can recover from experimentally induced central refractive errors after the restoration of unrestricted vision (Qiao-Grider et al., 2004; Siegwart & Norton, 1998; Troilo & Nickla, 2005; Troilo & Wallman, 1991; Wildsoet & Schmid, 2000). For example, following the onset of unrestricted vision, chickens, tree shrews, and monkeys with form-deprivation myopia exhibit dramatic reductions in axial growth rates. The eye's refractive status then becomes less myopic as a consequence of the reductions in corneal and lens power that normally take place during maturation. It has also been argued that in addition to the influence of visually guided mechanisms, the recovery from induced central refractive errors may be partially affected by mechanisms that are sensitive to ocular shape (e.g., Troilo & Wallman, 1991). However, it appears that the influence of potential shape-sensitive mechanisms can be overridden by vision-dependent mechanisms. For example, correcting the induced refractive errors with lenses or placing the animals in the dark disrupts recovery, which indicates that vision guides recovery from induced refractive errors (Amedo & Norton, 2012; Norton, Amedo, & Siegwart, 2006; Wildsoet & Schmid, 2000).

In addition to affecting central refractive development, vision can also influence the pattern of peripheral refractions. It has been shown that emmetropization, a process that requires vision, occurs for both central and peripheral refractions during normal development in monkeys (Hung et al., 2008). Moreover, form deprivation and optically imposed hyperopic defocus, in addition to producing central axial myopia, can alter the shape of the posterior globe and the pattern of peripheral refractions, specifically producing more prolate shaped eyes and relative peripheral hyperopia (Huang et al., 2009; Smith et al., 2010). Furthermore, hemi-field form deprivation and hemi-field optical defocus typically produce local refractive-error changes in the treated hemi-retina, through

* Corresponding author at: College of Optometry, University of Houston, 505 J. Armistead Building, Houston, TX 77204-2020, United States. Fax: +1 713 743 0965.
E-mail address: esmith@uh.edu (E.L. Smith III).

0042-6989/$ - see front matter © 2012 Elsevier Ltd. All rights reserved.
http://dx.doi.org/10.1016/j.visres.2012.09.002

mechanisms that integrate visual signals in a regionally restricted manner (Diether & Schaeffel, 1997; Smith et al., 2009, 2010; Wallman et al., 1987).

It is important to understand the factors that influence the pattern of peripheral refractive errors because the pattern of peripheral refractions can influence central refractive development and the pattern of peripheral refractions may be a predictor and/or risk factor for the development of central refractive errors (Hoogerheide, Rempt, & Hoogenboom, 1971; Mutti et al., 2007; Smith, 2011; Stone & Flitcroft, 2004; Wallman & Winawer, 2004). As mentioned above, young animals can recover from experimentally induced central refractive errors after the restoration of unrestricted vision. However, it is not known whether recovery also occurs in the periphery. Determining whether changes in ocular shape and the pattern of peripheral refractions occur during recovery will provide further insight into the role of vision on refractive development. This study aimed to determine whether the eyes of young monkeys with vision-induced central axial myopia can recover from the concomitant peripheral refractive errors and to characterize the alterations in ocular shape that occur during the recovery from central myopia.

2. Methods

2.1. Subjects

The subjects were infant rhesus monkeys (*Macaca mulatta*) that were obtained at approximately 2–3 weeks of age and housed in our primate nursery that was maintained on a 12-h light/12-h dark cycle (Smith & Hung, 1999). All rearing and experimental procedures were reviewed and approved by the University of Houston's Institutional Animal Care and Use Committee and were in compliance with the ARVO Statement for the Use of Animals in Ophthalmic and Vision Research.

Recovery from experimentally induced myopia was investigated longitudinally in 12 monkeys that had developed at least 0.50 D of myopic anisometropia in response to either lens-induced hyperopic defocus or form deprivation. Monocular hyperopic defocus was produced in six of the experimental monkeys by securing a −3.0 D spectacle lens in front of their treated eyes (−3.0 D monkeys) (Smith et al., 2010). Monocular form deprivation was imposed on another six monkeys by fitting a diffuser spectacle lens in front of their treated eyes (FD monkeys) (Smith et al., 2007). The diffuser lenses consisted of a zero-powered carrier lens covered with a commercially available occlusion foil (“LP” or “light perception” Bangerter Occlusion Foils; Fresnel Prism and Lens Co., Prairie, MN). For both treatment groups, clear, zero-powered lenses were secured in front of their fellow eyes. The lens-rearing regimens were started at 22 ± 2 days of age, and the monkeys wore the treatment lenses continuously until 158 ± 17 days of age. Subsequently, the lenses were removed and the animals were allowed unrestricted vision. The recovery period extended until at least 340 days of age for all of the treated monkeys. Control data were obtained from 10 monkeys; nine of the control monkeys were raised with unrestricted vision, and one wore plano lenses over both eyes. The data for the FD and −3.0 D monkeys obtained at the end of the lens-rearing period, and for six of the normal monkeys obtained at ages corresponding to the end of the lens-rearing period have been previously reported (Huang et al., 2009; Smith et al., 2010).

2.2. Ocular biometry

The biometry measurements were performed every 2–4 weeks from the start of lens wear throughout the treatment and recovery periods. To make the ocular measurements, the monkeys were anesthetized with an intramuscular injection of ketamine hydrochloride (15–20 mg/kg) and acepromazine maleate (0.15–0.2 mg/kg). The cornea was anesthetized with 1–2 drops of 0.5% tetracaine hydrochloride. Cycloplegia was produced with 1–2 drops of 1% tropicamide that were topically instilled in each eye 20–30 min before retinoscopy.

Two experienced observers independently determined the refractive errors of each eye by streak retinoscopy using hand-held trial lenses. The results were averaged (Harris, 1988) and specified as spherical-equivalent, spectacle-plane refractive corrections. Refractions were measured longitudinally along the pupillary axis and 15° intervals along the horizontal meridian out to eccentricities of 45° (Hung et al., 2008).

Ocular axial dimensions were measured along the pupillary axis by A-scan ultrasonography implemented with a 12-MHz transducer (OTI Scan 1000; OTI Ophthalmic Technologies, Inc., ON, Canada). Corneal curvature was measured with a hand-held keratometer (Alcon Auto-keratometer; Alcon Systems Inc., St. Louis, MO). To assess the shape of the peripheral cornea, corneal *Q*-values were obtained from the −3.0 D monkeys with a video topographer (EyeSys 2000; EyeSys Technologies Inc., Houston, TX). The topographer was not available to assess the corneas of the FD monkeys.

2.3. Magnetic resonance image acquisition

Magnetic resonance imaging (MRI) was performed on five of the −3.0 D monkeys near the end of the lens-rearing period (139–180 days of age) and later during the recovery period (289–379 days of age). MRIs were obtained with a 7 T horizontal bore scanner (Bruker Biospec USR 70/30; Bruker, Karlsruhe, Germany). The details of the MRI procedures have been described elsewhere (Huang et al., 2009; Smith et al., 2009, 2010).

The animals were anesthetized with 2% isoflurane gas anesthesia. After delimiting the position of the monkey's eyes with the initial tripilot scan, magnetic field homogeneity was optimized using a localized shimming procedure (point resolved spectroscopy). T_2-weighted images were obtained to enhance the contrast between the fluids and tissues of the eye. The repetition times and effective echo times of the scans were 1000 ms and 169–179 ms, respectively. The spatial resolution of the axial images was $0.195 \times 0.195 \times 0.5$ mm in the horizontal plane.

The acquired axial MR images were reconstructed using in-house software (MATLAB; MathWorks, Natick, MA), which interpolated between the axial image slices to produce a uniform resolution of 0.195 mm in the three-dimensional matrix. The software identified the axial image slice that contained the greatest lens thickness in the interpolated stack for measuring the ocular dimensions. The approximate optical axis of the eye was defined as the perpendicular through the midpoint of the line connecting the equatorial poles of the lens. The intersection of the presumed optical axis and the posterior lens surface was considered to be the approximate position of the second nodal point and was used as the reference for specifying retinal eccentricities. The primary measure of interest was vitreous chamber depth, defined as the distance between the approximate position of the second nodal point and the retina. Vitreous chamber depth in the horizontal meridian was determined as a function of eccentricity in 15° intervals to eccentricities of 45°. As we have previously reported (Huang et al., 2009), the vitreous chamber depths measured along the presumed optical axis by our MRI methods and traditional A-scan ultrasonography measures were highly correlated and comparable.

Axial length and equatorial diameter were also measured in the horizontal MRI plane. Axial length was defined as the distance from the anterior corneal surface to the retina along the presumed optical axis. Equatorial diameter was defined as the greatest dis-

tance between the nasal and the temporal retinas measured along a line perpendicular to the presumed optical axis.

2.4. Statistical analysis

Mixed-design, repeated measures ANOVAs (SuperANOVA; Abacus Concepts, Inc., Berkeley, CA) and multiple comparisons were used to detect if there were differences in refractive errors as a function of eccentricity between eyes and between subject groups (i.e., differences in the patterns of peripheral refraction). Probability values were adjusted with the Geisser–Greenhouse correction (Keselman, Algina, & Kowalchuk, 2001). When no significant eccentricity-dependent differences between treated and fellow eyes were found, power analyses were performed (G* power 3.1.2; Franz Faul, University of Kiel, Germany) (Faul et al., 2009) to calculate the minimum effect sizes that the repeated measures ANOVAs were likely to detect. Specifically, for the −3.0 D monkeys, eccentricity-dependent differences of 0.75 D between the treated and fellow eyes could be detected with powers greater than 0.9; whereas for the FD monkeys, primarily because of greater inter-subject variability, similar comparisons could detect eccentricity-dependent differences of 1.5 D (start of treatment) and 1 D (during recovery) with powers greater than 0.9. Paired *t*-tests were used to compare individual central refractive errors and ocular components between treated and fellow eyes. When data are reported as means, the variability of the data is expressed as standard errors. The threshold for significance was set at $P < 0.05$ for each analysis.

3. Results

The longitudinal changes in the central and peripheral refractions of the normal monkeys are shown in Fig. 1. The top row of graphs (A–C) shows the average spherical-equivalent refractive corrections plotted as a function of eccentricity. To illustrate the differences in the patterns of peripheral refraction between the two eyes, the bottom row shows the relative interocular differences in refractive error along the horizontal meridian for individual monkeys (right eye–left eye). Specifically, for the lower graphs (D–F), the data for each eye were first normalized to that eye's central refraction and then the relative refractions for the left eyes were subtracted from those for the right eyes at each eccentricity.

At ages corresponding to the start of the lens-rearing period (26 ± 5 days), the normal monkeys exhibited comparable amounts of moderate hyperopia along the pupillary axes in both eyes (Fig. 1A and D, right eye = +4.20 ± 1.76 D, left eye = +4.09 ± 1.79 D; $T = 1.45$, $P = 0.182$), and the patterns of peripheral refractions in the two eyes were well matched ($F = 0.33$, $P = 0.78$). As previously reported (Hung et al., 2008), the peripheral refractive errors were in general less hyperopic than the central refraction, particularly in the nasal visual field. With age, the degree of central hyperopia decreased and the peripheral refractions became more symmetrical along the horizontal meridian, exhibiting low degrees of relative peripheral myopia in both the nasal and temporal visual fields (Fig. 1B and C). A key point is that the central and peripheral refractions were very comparable in the two eyes throughout the observation period. Specifically, at ages corresponding to the end of the lens-rearing period (Fig. 1B and E, 151 ± 13 days), there were no significant interocular differences in the central (right eye = +1.85 ± 0.65 D, left eye = +2.06 ± 0.56 D; $T = -1.86$, $P = 0.10$) or peripheral refractions ($F = 0.40$, $P = 0.70$). At ages corresponding to end of the recovery period (Fig. 1C and F, 313 ± 18 days), the average central refractions were +1.74 ± 0.38 D and +1.78 ± 0.39 D for the right and left eyes, respectively ($T = -0.59$, $P = 0.57$), and there were no significant differences in the pattern of peripheral refractions between the two eyes ($F = 0.72$, $P = 0.53$). The vitreous chamber depths were also very similar in the two eyes throughout the observation period, specifically at ages corresponding to the start of the lens-rearing period (right eye = 8.67 ± 0.32 mm, left eye = 8.69 ± 0.31 mm; $T = -1.93$, $P = 0.09$), the end of the lens-rearing period (right eye = 10.14 ± 0.50 mm, left eye = 10.14 ± 0.51 mm; $T = 0.28$, $P = 0.79$), and the end of the recovery period (right eye = 10.77 ± 0.52 mm, left eye = 10.80 ± 0.53 mm; $T = -1.78$, $P = 0.11$).

As documented in previous studies (Huang et al., 2009; Smith et al., 2010), during the lens-rearing period, the treated eyes of the FD and −3.0 D monkeys developed less hyperopic/more myopic refractive errors than their fellow eyes and the degree of relative myopia decreased with eccentricity, i.e., the treated eyes also exhibited relative peripheral hyperopia. However, following the onset of unrestricted vision, the treated eyes of both the FD and −3.0 D monkeys demonstrated a substantial ability to recovery from the experimentally induced refractive errors. Fig. 2 shows longitudinal refractive error and vitreous chamber data for two representative FD (panels 2A and B) and −3.0 D monkeys (panels 2C and D). In each of the four panels, the top row of plots illustrates the patterns of peripheral refractive errors along the horizontal meridian obtained at various times during the recovery period, beginning with the onset of unrestricted vision (left most plots). In the lower graphs in each panel, vitreous chamber depth is plotted as a function of age for the treated (filled symbols) and fellow eyes (open symbols). In both subject groups, the onset of lens/diffuser wear produced a relative increase in the vitreous chamber elongation rates of the treated eyes, which resulted in the central myopia and relative peripheral hyperopia observed at the end of the treatment period. Following the onset of unrestricted vision, there was a relative decrease in the axial elongation rates of the treated eyes. As previously reported (Qiao-Grider et al., 2004), the concomitant decrease in the degree of central myopia in the treated eyes came about primarily as a result of the continued maturational decreases in corneal and lens power. Once isometropia was re-established, the two eyes subsequently exhibited similar vitreous chamber elongation rates. The key point is that the pattern of peripheral refractions in the treated eyes also changed over time. There were systematic reductions in the degree of relative peripheral hyperopia in the treated eyes, so that by the end of the recovery period the patterns of peripheral refractions were well matched in the two eyes with both eyes exhibiting moderate degrees of central hyperopia and primarily relative peripheral myopia.

Figs. 3 and 4 summarize the refractive-error changes for the FD and −3.0 D monkeys, respectively. The format of the figures is similar to that of Fig. 1, except that the relative interocular differences were designated as treated eye–fellow eye (versus right eye–left eye in Fig. 1). Data are shown for the start of the treatment period (A and D), the end of the treatment period (B and E), and the end of the recovery period (C and F). As in the normal subject group, at the start of the treatment period, the two eyes of the experimental monkeys exhibited similar degrees of central hyperopia and the patterns of peripheral refractions were well matched in the two eyes (Fig. 3A: $F = 0.80$, $P = 0.52$; Fig. 4A: $F = 3.36$, $P = 0.06$). At the end of the treatment period, the interocular differences in central refraction for the FD monkeys ranged from −2.50 to −8.00 D and the average degree of anisometropia (treated eye–fellow eye) was −5.32 ± 2.09 D. In addition, the patterns of peripheral refractions in the treated eyes of the FD monkeys were significantly different from those observed in their fellow eyes (Fig. 3B: $F = 7.41$, $P = 0.02$). For the −3.0 D monkeys, the interocular differences in central refraction were, as expected, smaller than those in FD monkeys ($T = 3.84$, $P = 0.01$), ranging from −0.60 to −3.27 D, with an average anisometropia (treated eye–fellow eye) of −2.10 ± 0.94 D. The overall pattern of peripheral refractions in the treated eyes

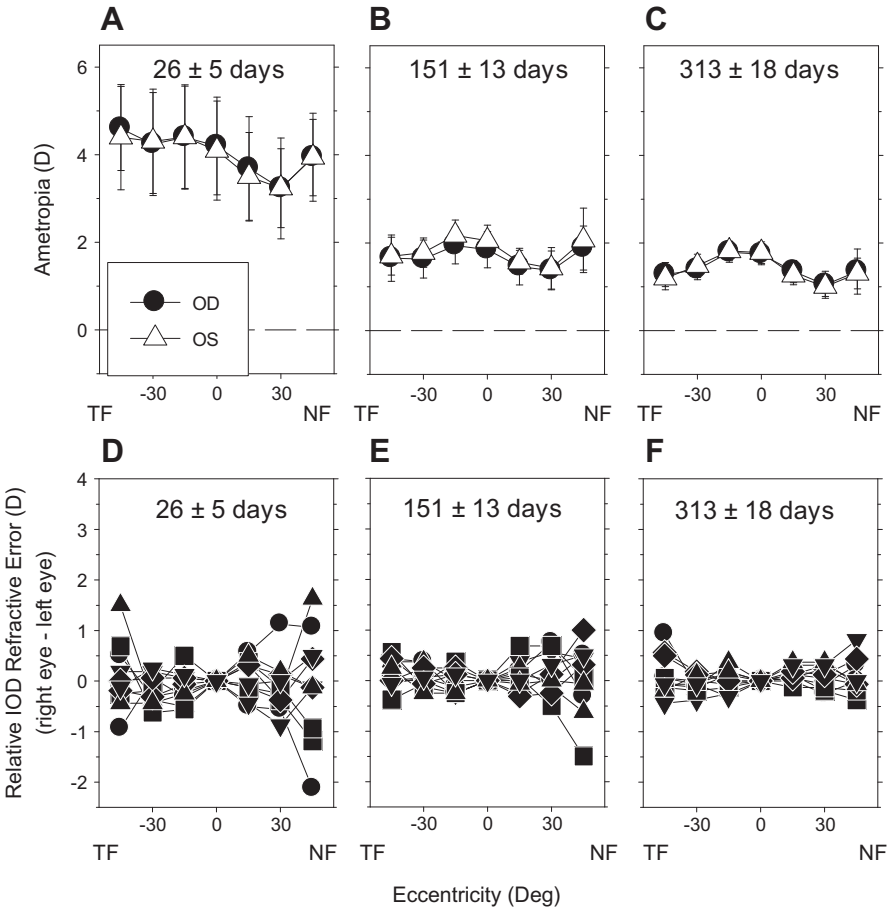

Fig. 1. The average spherical-equivalent refractive corrections (A–C) and individual normalized relative interocular differences (right eye–left eye) in spherical-equivalent refractive corrections (D–F) plotted as a function of eccentricity for the 10 control monkeys. The filled and open symbols in plots A–C represent the right and left eyes, respectively; each symbol shape in plots D–F represents an individual monkey. The data were obtained at ages corresponding to the start of the lens-rearing period (A and D), the end of the lens-rearing period (B and E), and the end of the recovery period (C and F), respectively. Error bars represent ±2 standard errors. TF = Temporal Field; NF = Nasal Field.

of the −3.0 D monkeys, was not significantly different from that in their fellow eyes (Fig. 4B: $F = 4.88$, $P = 0.06$). However, when the data from the monkey that developed the smallest anisometropia (−0.60D; the other five −3.0 D monkeys developed anisometropias of −1.50 D or greater) were excluded, the patterns of peripheral refractions in the treated and fellow eyes were significantly different ($F = 9.30$, $P = 0.02$). Specifically, as in the FD monkeys, the interocular differences in refractive error were greatest in the central retina and near nasal field and then decreased with eccentricity. With the onset of unrestricted vision, the degree of central myopia and relative peripheral hyperopia decreased in both treatment groups, and by the end of the recovery period, similar patterns of peripheral refractive errors were re-established in the treated and fellow eyes (Fig. 3C: $F = 2.76$, $P = 0.13$; Fig. 4C: $F = 1.70$, $P = 0.23$).

The relative interocular difference plots in the lower rows of Figs. 3 and 4 confirm on an individual basis that the patterns of the peripheral refractive errors were very similar in the two eyes of the experimental monkeys at the beginning of the treatment period and at the end of the recovery period. However, at the end of the lens-rearing period, the monkeys exhibited relative peripheral hyperopia in their treated eyes and the degree of relative hyperopia generally increased as a function of eccentricity. The patterns of interocular differences in spherical-equivalent refractive corrections for the experimental monkeys were comparable to those of normal monkeys at the start of the treatment period (FD monkeys: $F = 0.31$, $P = 0.82$; −3.0 D monkeys: $F = 0.93$, $P = 0.43$) and at the end of the recovery period (FD monkeys: $F = 3.12$, $P = 0.06$; −3.0 D monkeys: $F = 1.02$, $P = 0.39$), but were significantly different from those of normal monkeys at the end of the treatment period (FD monkeys: $F = 10.18$, $P = 0.0012$; −3.0 D monkeys: $F = 4.29$, $P = 0.02$).

As shown in Fig. 2, the changes in central refractive errors were associated with changes in central vitreous chamber depth. At the beginning of the treatment period, the central vitreous chamber depths were comparable in the two eyes of the FD (treated eye = 8.63 ± 0.34 mm, fellow eye = 8.68 ± 0.31 mm; $T = -1.20$, $P = 0.29$) and −3.0 D monkeys (treated eye = 8.58 ± 0.33 mm, fellow eye = 8.57 ± 0.31 mm; $T = 1.04$, $P = 0.35$). At the end of the treatment period, the central vitreous chamber depths of the treated eyes were significantly longer than those for their fellow eyes (FD monkeys: treated eye = 11.14 ± 0.75 mm, fellow eye = 10.17 ± 0.59 mm, $T = 4.23$, $P = 0.008$; −3.0 D monkeys: treated eye = 10.42 ± 0.63 mm, fellow eye = 10.00 ± 0.56 mm, $T = 5.59$, $P = 0.003$). During the recovery period, the vitreous chamber depths of the fellow control eyes caught up with those for the treated eyes and at the end of the observation period, the central vitreous chamber depths in the treated and fellow eyes were similar. (FD monkeys: treated eye = 11.40 ± 0.83 mm, fellow eye = 11.17 ± 0.90 mm, $T = 1.38$, $P = 0.23$; −3.0 D monkeys: treated eye = 10.94 ± 0.36 mm, fellow eye = 10.88 ± 0.38 mm, $T = 1.17$, $P = 0.30$). Additionally, the corneal powers were significantly higher in the

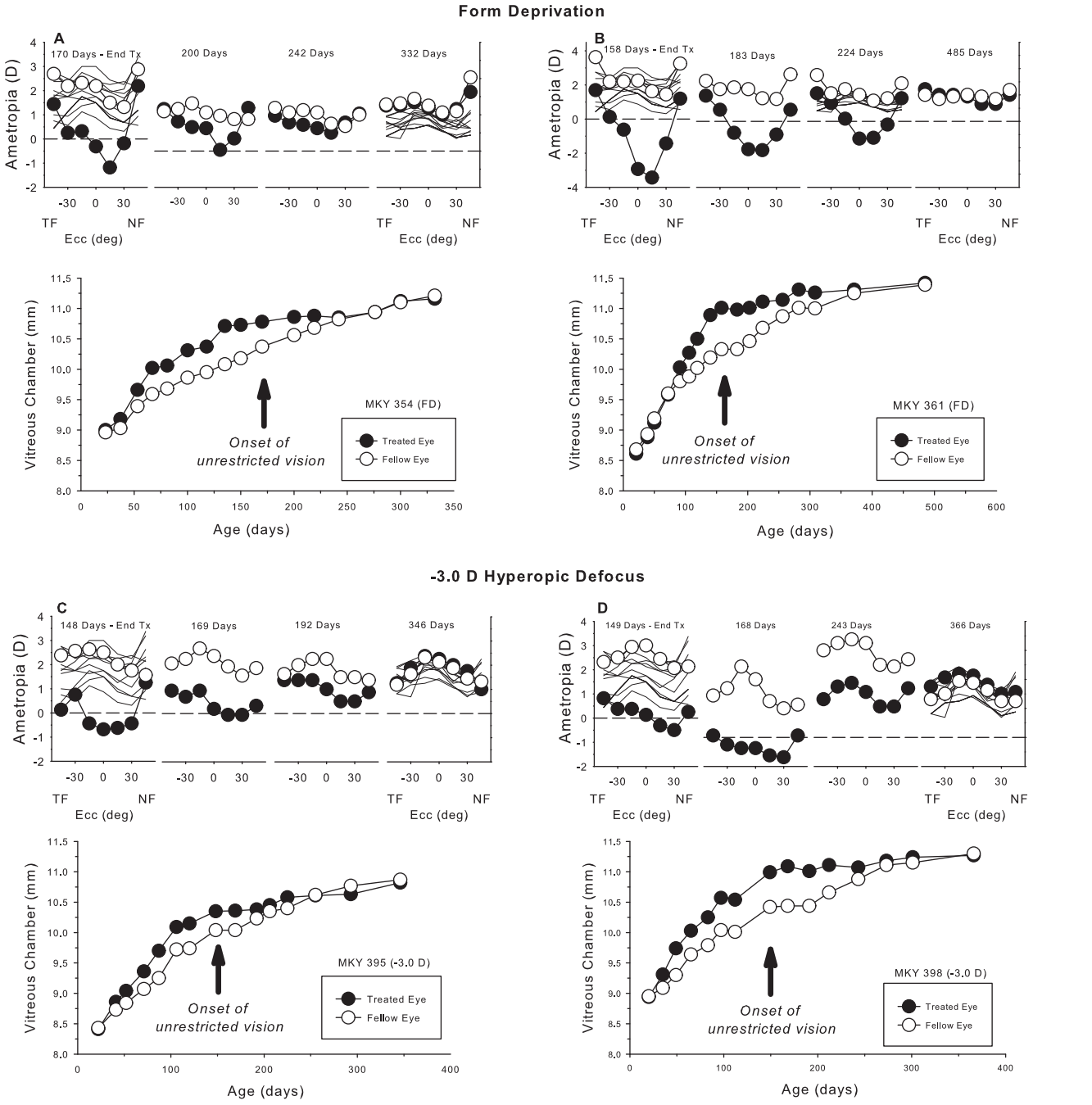

Fig. 2. Refractive errors plotted as a function of visual field eccentricity at different times during the recovery period (top panels) and corresponding changes in vitreous chamber depth plotted as a function of age (bottom panels) for two representative FD monkeys (A and B) and two −3.0 D monkeys (C and D). The filled and open symbols represent the treated and fellow eyes, respectively. The thin lines in the top rows of plots represent individual normal monkeys (n = 10) at ages corresponding to when the data were collected for the experimental monkeys. TF = Temporal Field; NF = Nasal Field. Ecc (deg) = Eccentricity (deg).

treated eyes of the FD monkeys at the end of the treatment period (treated eye = 55.47 ± 1.65 D, fellow eye = 54.66 ± 1.90 D, T = 4.32, P = 0.008), but not at the end of the recovery period (treated eye = 53.19 ± 1.95 D, fellow eye = 53.16 ± 1.98 D, T = 0.12, P = 0.91, P > 0.05). On the other hand, the −3.0 D monkeys did not show any significant interocular differences in central corneal powers at the end of the treatment or recovery periods (end of treatment: treated eye = 55.10 ± 1.36 D, fellow eye = 55.21 ± 1.56 D, T = −0.40, P = 0.71; end of recovery: treated eye = 52.99 ± 1.05 D, fellow eye = 53.21 ± 1.39 D, T = −0.83, P = 0.45), probably because the magnitude of induced myopia was smaller than that produced by form deprivation. Furthermore, there were no significant differences in corneal Q-values between the treated and fellow eyes of the −3.0 D monkeys during the recovery period (treated eye = −0.10 ± 0.20, fellow eye = −0.13 ± 0.14, T = 0.82, P = 0.45).

In the −3.0 D monkeys, the alterations in the pattern of the peripheral refractions during the recovery period were associated with changes in the shape of the posterior globe. The top row of Fig. 5 shows the MR images obtained in the horizontal meridian at the end of lens-rearing period and during the recovery period for two of the −3.0 D monkeys. The middle row of Fig. 5 shows the corresponding superimposed outlines of the MR images for

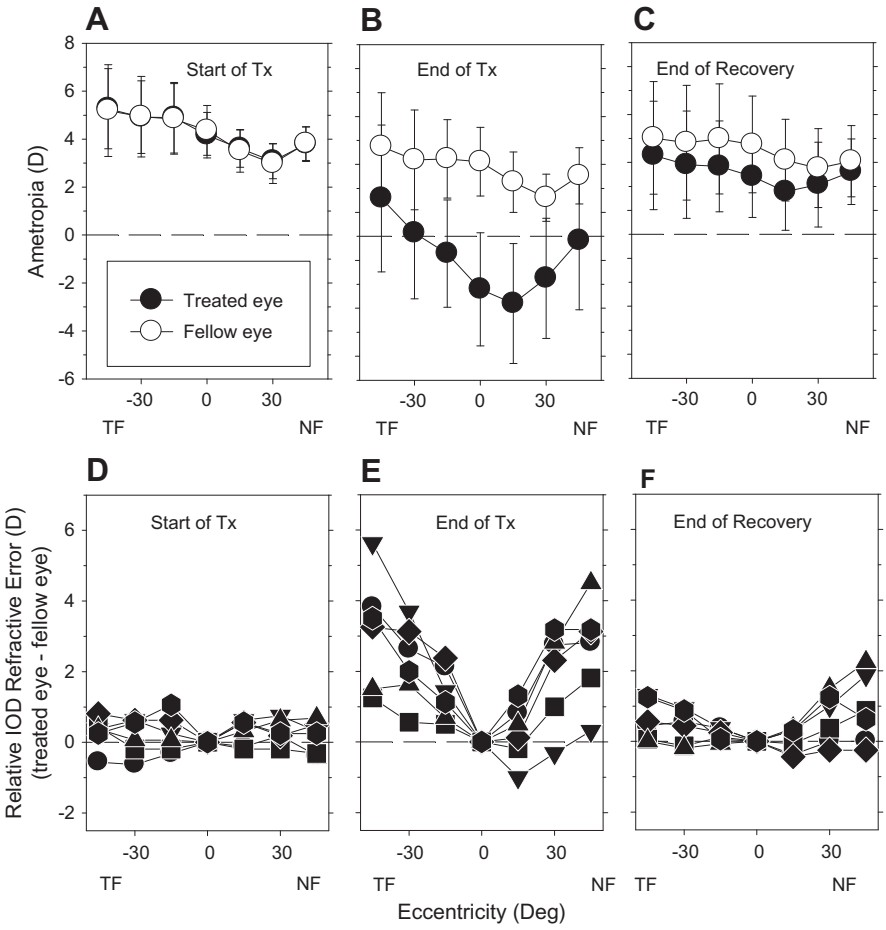

Fig. 3. The average spherical-equivalent refractive corrections (A–C) and individual normalized relative interocular differences (treated eye–fellow eye) in spherical-equivalent refractive corrections (D–F) plotted as a function of eccentricity for the six FD monkeys. The filled and open symbols in plots A–C represent the treated and fellow eyes, respectively. See Fig. 1 for details.

the treated (left) and fellow eyes (right) that were obtained at the end of lens-rearing period (red line) and during the recovery period (blue line). The bottom row shows vitreous chamber depths obtained from the MR images plotted as a function of retinal eccentricity for the treated (filled symbols) and fellow eyes (open symbols). The circles and triangles represent data obtained at the end of lens-rearing period and during the recovery period, respectively. After the removal of the treatment lenses, both the treated and fellow eyes enlarged during the recovery period, primarily as a result of elongation of the vitreous chamber. However, the patterns of enlargement were different between the treated and fellow eyes. The fellow eyes exhibited more uniform elongation across the central and peripheral posterior globe, whereas the treated eyes showed more elongation in the periphery than in the central region, resulting in a less prolate eye shape compared to the ocular contour exhibited at the end of the lens-rearing period. For example, for the fellow eye of subject MKY 395 (Fig. 5 left), the vitreous chamber elongation during recovery period was 0.75 mm along the presumed optical axis versus 0.84 mm and 0.69 mm at the 45° nasal and temporal retinal eccentricities. In contrast, the increase in vitreous chamber depth of the treated eye was 0.15 mm in the central retina versus 0.60 mm and 0.48 mm at the 45° nasal and temporal retinal eccentricities, respectively.

Fig. 6 shows the average interocular differences (treated eye–fellow eye) in vitreous chamber depth plotted as a function of retinal eccentricity obtained at the end of the lens-rearing period and near the end of the recovery period for the five −3.0 D monkeys for which MRI data were acquired. On average, at the end of the lens-rearing period (filled circles), the treated eyes were longer than their fellow eyes, and the differences in vitreous chamber depth were more prominent in the central than in the peripheral retina. In contrast, near the end of the recovery period (open triangles), the vitreous chamber depths were similar in the two eyes across the retina. The overall patterns of interocular differences in vitreous chamber depth as a function of retinal eccentricity were not significantly different between the end of the lens-rearing period and the end of the recovery period ($F = 1.19$, $P = 0.34$). However, post hoc tests revealed that the differences were significant ($P < 0.05$) at all eccentricities except for the 45° temporal ($F = 3.83$, $P = 0.09$) retinal eccentricity.

Fig. 7 shows the axial length/equatorial diameter (AL/ED) ratios for the treated (filled symbols) and fellow eyes (open symbols) for the five −3.0 D monkeys for which MRI data were acquired. At the end of the lens-rearing period, the average AL/ED ratio of the treated eyes was greater than that of the fellow eyes (0.974 ± 0.013 versus 0.963 ± 0.016), indicating that the treated eyes were more prolate in shape, although the difference was not statically significant ($T = 1.45$, $P = 0.22$). In contrast, following recovery, the average AL/ED ratio was slightly greater in the fellow eyes (0.961 ± 0.015 for the fellow eyes versus 0.958 ± 0.018 for the treated eyes; $T = -0.48$, $P = 0.66$). Inspecting individual data revealed that during the recovery period, the AL/ED ratio remained relatively unchanged in the fellow eyes, while the AL/ED ratios in the

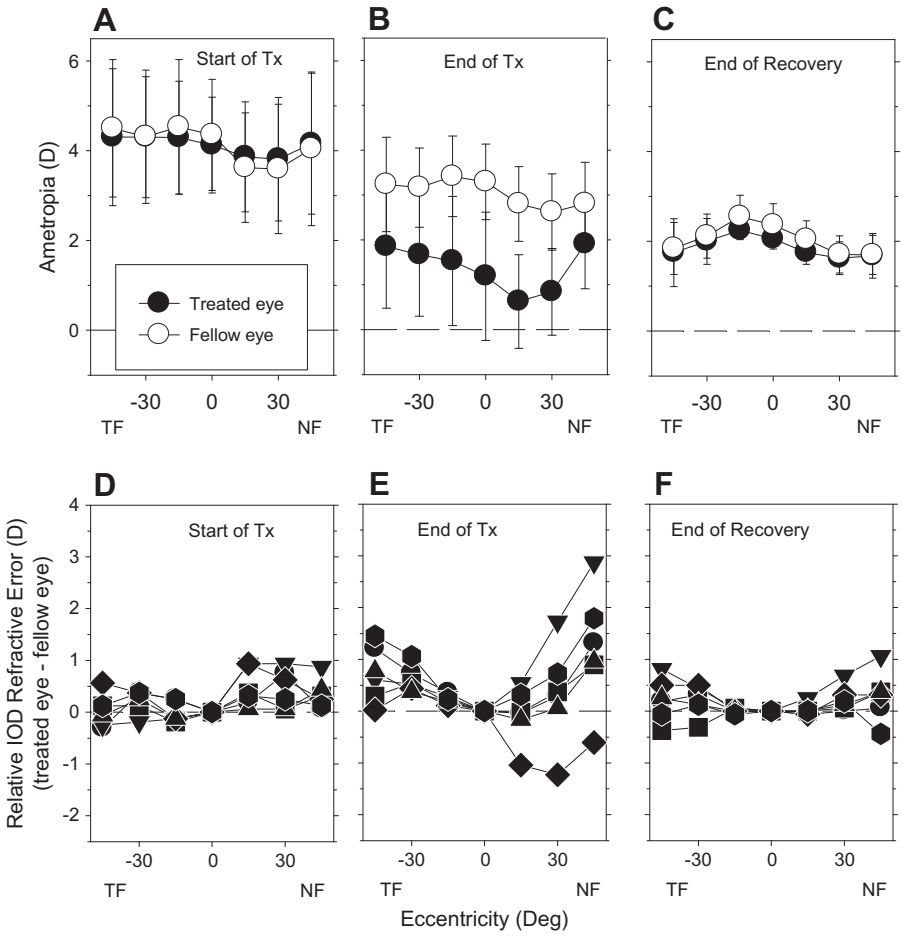

Fig. 4. The average spherical-equivalent refractive corrections (A–C) and individual normalized relative interocular differences (treated eye–fellow eye) in spherical-equivalent refractive corrections (D–F) plotted as a function of eccentricity for the six −3.0 D monkeys. The filled and open symbols in plots A–C represent the treated and fellow eyes, respectively. See Fig. 1 for details.

treated eyes decreased in four of the five monkeys, indicating that the eyes became more oblate during the recovery period.

4. Discussion

Our experiments show that following the onset of unrestricted vision, the eye can recover from experimentally induced central and peripheral refractive errors. The results extend previous findings on the recovery of central refractive errors in infant monkeys (Qiao-Grider et al., 2004) to include the alterations in peripheral refraction that develop in concert with central refractive errors. Consistent with previous observations that vision-induced alterations in peripheral refractions reflect corresponding alterations in ocular shape (Huang et al., 2009), our experiments indicate that the recovery of peripheral refraction is also associated with changes in the shape of the posterior globe.

Although the mechanisms that mediate the effects of form deprivation and optically induced defocus on refractive development are not identical (e.g. Bartmann et al., 1994; Kee, Marzani, & Wallman, 2001; Schaeffel et al., 1994), the changes in refraction that took place during the treatment period were qualitatively similar in the FD and −3.0 D monkeys. As expected, the degree of central form-deprivation myopia was, on average, larger than that produced by −3 D of hyperopic defocus. However, at the end of the treatment period the patterns of interocular differences in refractive error as a function of eccentricity were similar in the FD and −3.0 D monkeys. The fact that the patterns of peripheral refraction were comparable suggests that the factors that lead to the development of relatively prolate-shaped eyes and relative peripheral hyperopia are common to both form-deprivation myopia and negative-lens-induced myopia.

Given the similarities in the patterns of refraction at the end of the treatment period, it is not surprising that the FD and −3.0 D monkeys exhibited similar recovery patterns. In essence, both subject groups had similar visual experiences during the recovery period. Although it is not always possible to confidently identify the sign of defocus in animals unless the viewing distance and accommodation can be controlled, it is reasonable to assume that in both the FD and −3.0 D monkeys, the primary stimulus for recovery was myopic defocus in the treated eyes, which varied systematically with eccentricity. In both subject groups, the treated eyes were more myopic or less hyperopic than their fellow control eyes. It is likely that the treated eyes experienced primarily myopic defocus, at least at the start of the recovery period, because accommodation is highly correlated in the two eyes of monkeys (Troilo, Totonelly, & Harb, 2009) and it is likely that the animals fixated with their fellow eyes. In particular in the FD animals, the treated eyes were probably severely amblyopic at the end of the treatment period (Smith, Hung, & Harwerth, 2000), forcing the animals to fixate with their fellow eyes. Similarly it is likely that the −3.0 D monkeys that did not exhibit complete compensation by the end

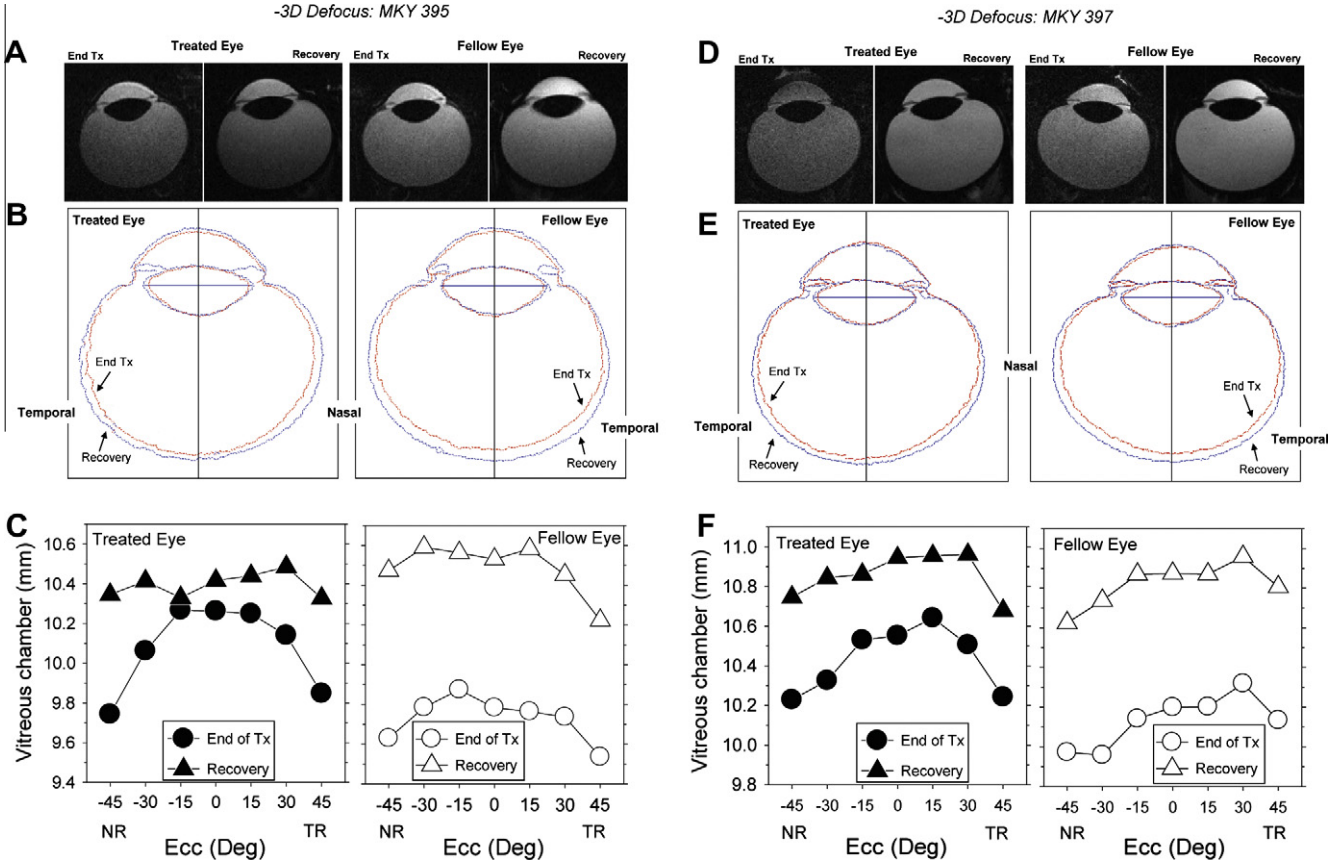

Fig. 5. Figures A and D shows the horizontal MR images obtained at the end of the lens-rearing period (left) and during the recovery period (right) for two representative −3.0 D monkeys. Figures B and E show the corresponding superimposed outlines of the MR images for the treated (left) and fellow eyes (right) that were obtained at the end of the lens-rearing period (red line) and during the recovery period (blue line). The superimposed images were aligned using the lines that connected the equatorial poles of the crystalline lenses as a reference. Figures C and F shows vitreous chamber depth obtained from the MR images (A and D) plotted as a function of retinal eccentricity for the treated (filled symbols) and fellow eyes (open symbols). Circles and triangles represent data obtained at the end of the lens-rearing period and during the recovery period, respectively. TF = Temporal Field; NF = Nasal Field. Ecc (deg) = Eccentricity (deg).

of the treatment period also preferred to fixate with their fellow eyes. The observed reductions in central vitreous chamber elongation rate that took place at the onset of the recovery period in both the FD and −3.0 D monkeys reinforce the idea that the treated eyes of the experimental monkeys experienced myopic defocus at the start of the recovery period.

As illustrated in Figs. 2 and 5, the recovery in central and peripheral refractions was primarily axial in nature. In the FD monkeys, a small degree of the recovery of central refractions can be attributed to a greater decrease in central corneal power in the

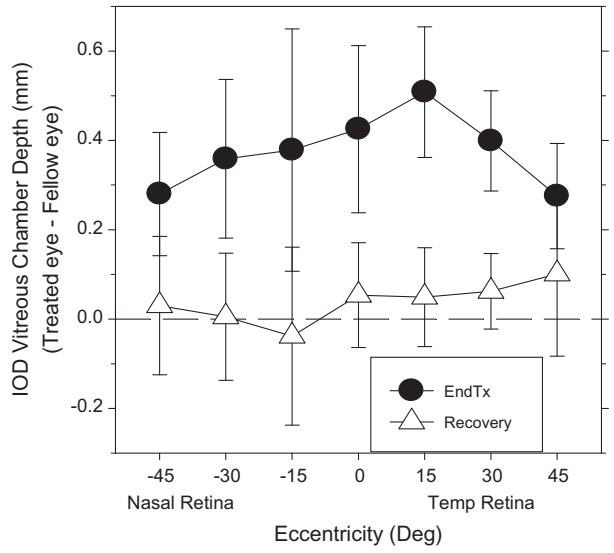

Fig. 6. The average interocular differences (treated–fellow eye) in vitreous chamber depth plotted as a function of visual field eccentricity obtained at the end of the lens-rearing period (filled circles) and during the recovery period (open triangles) for the five −3.0 D monkeys for which MRI data were acquired. Error bars represent ±2 standard errors.

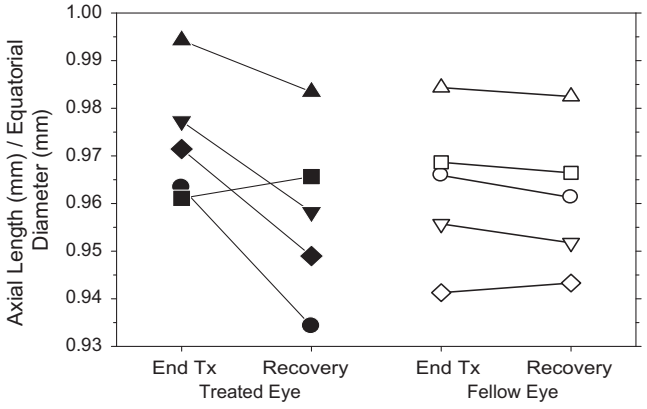

Fig. 7. The axial length/equatorial diameter (AL/ED) ratios for the treated (filled symbols) and fellow eyes (open symbols) for the five −3.0 D monkeys for which MRI data were acquired. Each symbol shape represents an individual subject.

treated versus the fellow control eyes (about 0.8 D). Although we did not attempt to assess lens power, we previously failed to observe any interocular differences in lens power at the end of the treatment period in either lens- or diffuser-reared monkeys (Huang et al., 2009; Qiao-Grider et al., 2010). In this respect, there was also no evidence for interocular differences in the age-dependent changes in the ocular optical components in the −3.0 D monkeys during the recovery period. Moreover, assessment of corneal shape in the −3.0 D monkeys ruled out the possibility that changes in the pattern of peripheral refractions during the recovery period were due to alterations in corneal asphericity. Instead the recovery in the pattern of peripheral refractions appears to reflect regional variations in axial growth.

Several previous observations are in agreement with the idea that the changes in ocular shape and the pattern of peripheral refractions observed during the recovery period in this experiment were visually driven. For example, emmetropization, which has been shown to be a vision-dependent phenomenon (Norton & Siegwart, 1995; Smith, 1998, 2011; Wallman & Winawer, 2004; Wildsoet, 1997), occurs in both the central and peripheral retina (Hung et al., 2008). In this respect, it is reasonable to argue that the local, regionally selective retinal mechanisms that dominate the effects of vision on refractive develop (Diether & Schaeffel, 1997; Smith et al., 2009, 2010; Wallman et al., 1987) evolved to optimize the eye's effective refractive state across the retina. Probably the strongest evidence that the shape of the eye is regulated by visual experience, however, comes from experiments which show that imposing optical defocus over half of the retina produces changes in ocular shape and refractive error that are largely restricted to the treated hemi-retina and compensating in nature. The alterations in peripheral refraction that we observed during the recovery from diffuser and negative lens myopia appear to be analogous to those observed with imposed hemi-retinal defocus.

Some vision-induced changes in the pattern of peripheral refractions do not, however, appear to be compensatory. For example, full-field form deprivation results in central myopia and relative peripheral hyperopia. In our experiments, the strength of the diffusers that were employed to produce form deprivation were strong enough to eliminate growth regulating dioptric vergence signals across a very large part of the retina. In essence, the resulting axial growth was unregulated across the retina. Nevertheless the eyes still became more prolate in shape. However, in the case of negative-lens-induced central myopia, it could be argued that the resulting prolate shape changes and peripheral hyperopia were compensatory in nature. With low-powered negative lenses, the effective strength of the defocus signal decreases with eccentricity, perhaps as a result of the normal reduction in the spatial resolving capacity of retinal neurons (i.e., the effective depth of the focus increases with eccentricity). However, ablating the central 10–12 degrees of the retina, which would alter any eccentricity-dependent variations in growth signals between the fovea and near periphery, does not appear to alter the pattern of peripheral refractions observed in monkeys with negative-lens-induced central myopia (Smith, Hung, & Huang, 2009), possibly because the effective integration zones of local retinal mechanisms are large in comparison to the size of the foveal ablations.

A variety of non-visual explanations has also been put forward to potentially explain the prolate shape changes that are associated with the development of axial myopia. It has been hypothesized that eccentricity-dependent variations in the number or density of critical retinal neurons (in essence, variations in the sensitivity of local retinal mechanisms or the strength of their vision-induced signals), in critical choroidal or scleral components, or in the spatial integration properties of the local retinal mechanisms could contribute to the prolate alterations in ocular shape during myopia development (Atchison et al., 2004; McBrien, Cottriall, & Annies, 2001; Rada, Nickla, & Troilo, 2000; Wallman & Winawer, 2004). It has also been postulated that mechanical factors, both intraocular and extraocular, could affect ocular shape during refractive development (Atchison et al., 2004; Mathis & Schaeffel, 2010; Mutti et al., 2004). For example, it has been argued that anatomic constraints imposed by the orbit may enable the eye to elongate more easily in the axial direction. However, it is important to note that the prolate changes observed in this study developed during infancy when both the eye and orbit are actively growing. Thus, the nature of external forces is unknown, but probably different from that found in older animals and probably highly dynamic. Regardless, the nature of the ocular shape changes that occurred during recovery from negative-lens-induced myopia (Figs. 5 and 6) argues against simple mechanical factors playing a major role. In particular, we found greater elongation in the peripheral region during the recovery period than in the central retina, i.e., although the eyes were still increasing in axial length, the eyes became more oblate in shape. These results are important because they demonstrate that both prolate and oblate shape changes can take place during central axial elongation.

With respect to vision-dependent mechanisms, our results in both FD and −3.0 D monkeys emphasize that axial elongation is greatest in the central retinal area during the development of vision-induced myopia indicating that the effectiveness or strength of growth signals is greatest in the central retina. Moreover, during recovery the greatest reductions in growth were found in the central retina suggesting again that the effectiveness or strength of signals to reduce growth were greatest in the central retina. However, in the case of recovery from induced myopia, interpretation of the results is confounded by the fact that the degree of relative myopic defocus varied as a function of eccentricity. In terms of understanding the role of peripheral vision in the genesis of common central refractive errors and in the potential therapeutic benefits associated with manipulating peripheral vision, it will be important to develop a clear understanding of how signals across the retina are integrated to influence both local and overall ocular growth.

It seems likely that the shape of the posterior globe is affected by multiple factors during refractive development. Although questions remain concerning the exact mechanisms responsible for the changes in peripheral refraction and ocular shape during refractive development, our experiments show that young rhesus monkeys can recover from the central and peripheral refractive errors produced by early monocular form deprivation and hyperopic optical defocus. These results emphasize that the pattern of peripheral refractions is not constant and that the pattern of peripheral refractions observed in older subjects may not necessarily reflect the pattern of peripheral refractions at an earlier age.

Acknowledgments

This work was supported by NIH Grants EY-03611 and EY-07551 and funds from the Vision Cooperative Research Centre, Sydney, Australia.

References

Amedo, A. O., & Norton, T. T. (2012). Visual guidance of recovery from lens-induced myopia in tree shrews (*Tupaia glis belangeri*). *Ophthalmic and Physiological Optics, 32*(2), 89–99.

Atchison, D. A., Jones, C. E., Schmid, K. L., Pritchard, N., Pope, J. M., Strugnell, W. E., et al. (2004). Eye shape in emmetropia and myopia. *Investigative Ophthalmology and Visual Science, 45*(10), 3380–3386.

Bartmann, M., Schaeffel, F., Hagel, G., & Zrenner, E. (1994). Constant light affects retinal dopamine levels and blocks deprivation myopia but not lens-induced refractive errors in chickens. *Visual Neuroscience, 11*(2), 199–208.

Diether, S., & Schaeffel, F. (1997). Local changes in eye growth induced by imposed local refractive error despite active accommodation. *Vision Research, 37*(6), 659–668.

Faul, F., Erdfelder, E., Buchner, A., & Lang, A. G. (2009). Statistical power analyses using G*Power 3.1: Tests for correlation and regression analyses. *Behavior Research Methods, 41*(4), 1149–1160.

Harris, W. F. (1988). Algebra of sphero-cylinders and refractive errors, and their means, variance, and standard deviation. *American Journal of Optometry and Physiological Optics, 65*(10), 794–802.

Hoogerheide, J., Rempt, F., & Hoogenboom, W. P. (1971). Acquired myopia in young pilots. *Ophthalmologica, 163*(4), 209–215.

Howlett, M. H., & McFadden, S. A. (2009). Spectacle lens compensation in the pigmented guinea pig. *Vision Research, 49*(2), 219–227.

Huang, J., Hung, L. F., Ramamirtham, R., Blasdel, T. L., Humbird, T. L., Bockhorst, K. H., et al. (2009). Effects of form deprivation on peripheral refractions and ocular shape in infant rhesus monkeys (*Macaca mulatta*). *Investigative Ophthalmology and Visual Science, 50*(9), 4033–4044.

Hung, L. F., Crawford, M. L., & Smith, E. L. (1995). Spectacle lenses alter eye growth and the refractive status of young monkeys. *Nature Medicine, 1*(8), 761–765.

Hung, L. F., Ramamirtham, R., Huang, J., Qiao-Grider, Y., & Smith, E. L. 3rd, (2008). Peripheral refraction in normal infant rhesus monkeys. *Investigative Ophthalmology and Visual Science, 49*(9), 3747–3757.

Kee, C. S., Marzani, D., & Wallman, J. (2001). Differences in time course and visual requirements of ocular responses to lenses and diffusers. *Investigative Ophthalmology and Visual Science, 42*(3), 575–583.

Keselman, H. J., Algina, J., & Kowalchuk, R. K. (2001). The analysis of repeated measures designs: A review. *British Journal of Mathematical and Statistical Psychology, 54*(Pt 1), 1–20.

Mathis, U., & Schaeffel, F. (2010). Transforming growth factor-beta in the chicken fundal layers: An immunohistochemical study. *Experimental Eye Research, 90*(6), 780–790.

McBrien, N. A., Cottriall, C. L., & Annies, R. (2001). Retinal acetylcholine content in normal and myopic eyes: A role in ocular growth control? *Visual Neuroscience, 18*(4), 571–580.

Mutti, D. O., Hayes, J. R., Mitchell, G. L., Jones, L. A., Moeschberger, M. L., Cotter, S. A., et al. (2007). Refractive error, axial length, and relative peripheral refractive error before and after the onset of myopia. *Investigative Ophthalmology and Visual Science, 48*(6), 2510–2519.

Mutti, D. O., Mitchell, G. L., Jones, L. A., Friedman, N. E., Frane, S. L., Lin, W. K., et al. (2004). Refractive astigmatism and the toricity of ocular components in human infants. *Optometry and Vision Science, 81*(10), 753–761.

Norton, T. T., Amedo, A. O., & Siegwart, J. T. Jr., (2006). Darkness causes myopia in visually experienced tree shrews. *Investigative Ophthalmology and Visual Science, 47*(11), 4700–4707.

Norton, T. T., & Siegwart, J. T. Jr., (1995). Animal models of emmetropization: Matching axial length to the focal plane. *Journal of the American Optometric Association, 66*(7), 405–414.

Qiao-Grider, Y., Hung, L. F., Kee, C. S., Ramamirtham, R., & Smith, E. L. 3rd, (2004). Recovery from form-deprivation myopia in rhesus monkeys. *Investigative Ophthalmology and Visual Science, 45*(10), 3361–3372.

Qiao-Grider, Y., Hung, L. F., Kee, C. S., Ramamirtham, R., & Smith, E. L. 3rd, (2010). Nature of the refractive errors in rhesus monkeys (*Macaca mulatta*) with experimentally induced ametropias. *Vision Research, 50*(18), 1867–1881.

Rada, J. A., Nickla, D. L., & Troilo, D. (2000). Decreased proteoglycan synthesis associated with form deprivation myopia in mature primate eyes. *Investigative Ophthalmology and Visual Science, 41*(8), 2050–2058.

Schaeffel, F., Glasser, A., & Howland, H. C. (1988). Accommodation, refractive error and eye growth in chickens. *Vision Research, 28*(5), 639–657.

Schaeffel, F., Hagel, G., Bartmann, M., Kohler, K., & Zrenner, E. (1994). 6-Hydroxy dopamine does not affect lens-induced refractive errors but suppresses deprivation myopia. *Vision Research, 34*(2), 143–149.

Schaeffel, F., & Howland, H. C. (1991). Properties of the feedback loops controlling eye growth and refractive state in the chicken. *Vision Research, 31*(4), 717–734.

Shaikh, A. W., Siegwart, J. T., Jr., & Norton, T. T. (1999). Effect of interrupted lens wear on compensation for a minus lens in tree shrews. *Optometry and Vision Science, 76*(5), 308–315.

Siegwart, J. T., Jr., & Norton, T. T. (1998). The susceptible period for deprivation-induced myopia in tree shrew. *Vision Research, 38*(22), 3505–3515.

Smith, E. L. 3rd, (2011). Prentice Award Lecture 2010: A case for peripheral optical treatment strategies for myopia. *Optometry and Vision Science, 88*(9), 1029–1044.

Smith, E. L., 3rd, Huang, J., Hung, L. F., Blasdel, T. L., Humbird, T. L., & Bockhorst, K. H. (2009). Hemiretinal form deprivation: Evidence for local control of eye growth and refractive development in infant monkeys. *Investigative Ophthalmology and Visual Science, 50*(11), 5057–5069.

Smith, E. L., 3rd, & Hung, L. F. (1999). The role of optical defocus in regulating refractive development in infant monkeys. *Vision Research, 39*(8), 1415–1435.

Smith, E. L., 3rd, Hung, L. F., & Harwerth, R. S. (2000). The degree of image degradation and the depth of amblyopia. *Investigative Ophthalmology and Visual Science, 41*(12), 3775–3781.

Smith, E. L., 3rd, Hung, L. F., & Huang, J. (2009). Relative peripheral hyperopic defocus alters central refractive development in infant monkeys. *Vision Research, 49*(19), 2386–2392.

Smith, E. L., 3rd, Hung, L. F., Huang, J., Blasdel, T. L., Humbird, T. L., & Bockhorst, K. H. (2010). Effects of optical defocus on refractive development in monkeys: Evidence for local, regionally selective mechanisms. *Investigative Ophthalmology and Visual Science, 51*(8), 3864–3873.

Smith, E. L., 3rd, Ramamirtham, R., Qiao-Grider, Y., Hung, L. F., Huang, J., Kee, C. S., et al. (2007). Effects of foveal ablation on emmetropization and form-deprivation myopia. *Investigative Ophthalmology and Visual Science, 48*(9), 3914–3922.

Smith, E. L. 3rd, (1998). Environmentally induced refractive errors in animals. In M. Rosenfield & B. Gilmartin (Eds.), *Myopia and nearwork* (pp. 57–90). Oxford: Butterworth-Heinemann.

Stone, R. A., & Flitcroft, D. I. (2004). Ocular shape and myopia. *Annals of the Academy of Medicine, Singapore, 33*(1), 7–15.

Troilo, D., & Nickla, D. L. (2005). The response to visual form deprivation differs with age in marmosets. *Investigative Ophthalmology and Visual Science, 46*(6), 1873–1881.

Troilo, D., Totonelly, K., & Harb, E. (2009). Imposed anisometropia, accommodation, and regulation of refractive state. *Optometry and Vision Science, 86*(1), E31–39.

Troilo, D., & Wallman, J. (1991). The regulation of eye growth and refractive state: An experimental study of emmetropization. *Vision Research, 31*(7–8), 1237–1250.

Wallman, J., Gottlieb, M. D., Rajaram, V., & Fugate-Wentzek, L. A. (1987). Local retinal regions control local eye growth and myopia. *Science, 237*(4810), 73–77.

Wallman, J., & Winawer, J. (2004). Homeostasis of eye growth and the question of myopia. *Neuron, 43*(4), 447–468.

Whatham, A. R., & Judge, S. J. (2001). Compensatory changes in eye growth and refraction induced by daily wear of soft contact lenses in young marmosets. *Vision Research, 41*(3), 267–273.

Wildsoet, C. F. (1997). Active emmetropization – Evidence for its existence and ramifications for clinical practice. *Ophthalmic and Physiological Optics, 17*(4), 279–290.

Wildsoet, C. F., & Schmid, K. L. (2000). Optical correction of form deprivation myopia inhibits refractive recovery in chick eyes with intact or sectioned optic nerves. *Vision Research, 40*(23), 3273–3282.